Noncoherent MT-MFSK Signals With Diversity Reception in Arbitrarily Correlated and Unbalanced Nakagami-m Fading Channels

Ibrahim Ghareeb, *Member, IEEE*

***Abstract*—This paper studies the performance of diversity applied to an efficient modulation/coding scheme using M-ary frequency-shift keying (MFSK) signals, with postdetection noncoherent diversity reception and combining over slow nonselective arbitrarily correlated and unbalanced Nakagami-m fading channels, in which the diversity branches can have unequal signal-to-noise ratios (SNRs), as well as different severity parameter m. This modulation/coding scheme is referred to as multiple tone MFSK (MT-MFSK) and is implemented based on balanced incomplete block design (BIB-design) from combinatorial theory. In MT-MFSK modulation, the number of tones used to represent the signals set is reduced compared with the conventional MFSK modulation, and each MT-MFSK signal is represented by a number of distinct orthogonal tones selected according to BIB-design. This mechanism drastically increase the bandwidth efficiency of the modulated signal and allows the modulator to create implicit frequency diversity. In this paper, we show that by combining the implicit frequency diversity of MT-MFSK signals with the diversity reception introduced by employing multiple receiving antennas, substantial improvements in performance can be obtained. A noncoherent square-law combining (SLC) soft-decision receiver is introduced and a union bound expression for the average symbol error probability is obtained. The effects of arbitrarily values of fading severity parameter m and the arbitrarily correlation between the unbalanced L diversity channels are considered. The system performance is compared with that of the conventional MFSK system. The results show that this modulation/coding scheme creates a multiplicative diversity and, therefore, performs better than the conventional MFSK system in terms of power and bandwidth efficiency.**

***Index Terms*—Arbitrarily correlated and unbalanced Nakagami-m fading channels, M-ary frequency-shift keying (MFSK), multichannel diversity reception, multiple tone MFSK (MT-MFSK), postdetection diversity, square-law combining (SLC).**

I. Introduction

WIRELESS communication services are penetrating into our society at an explosive growth rate, and working toward specification of these services is ongoing. One key feature of future wireless communication systems is likely to be the availability of much higher data rates. Higher spectral efficiency and lower cost per transmitted bit are other key requirements. Multipath fading on wireless channels present a fundamental technical challenge to reliable communication, where errors occur frequently when the channel is in a deep fade. In this case, the communication between the transmitter and the receiver is degraded, and wireless channel does not readily accommodate rapid flow of data. However, if multiple receiving antennas are used, the receiver can be provided with several replicas of the information signal which have been subjected to different fading mechanisms, and an appropriate diversity combining method can restore the information and make the communication more reliable [1].

In some practical mobile systems, the fading statistics between the diversity paths may be correlated, which reduces diversity gain and must be taken into account in the system design. On this issue, the performance evaluation of M-ary frequency-shift keying (MFSK) signals over correlated Nakagami-fading channels with postdetection square-law combining (SLC) has been studied in [2]–[5]. A great deal of interest has recently raised in using algebraic tools to design modulation/coding schemes using MFSK signals. These schemes are naturally required to be suitable for fading channels [6]–[12]. The principal advantage of these modulation/coding schemes, is their ability to create implicit diversity to improve power efficiency without the customary bandwidth expansion introduced by the use of coding.

Multiple Tone MFSK (MT-MFSK) modulation is an integrated modulation/coding scheme designed for bandwidth constrained channels. In this modulation scheme, the number of tones used to represent the signals set is reduced compared with conventional MFSK modulation and, therefore, bandwidth efficiency is improved. In [6] and [7], the reduction in the number of tones is based on the use of permutations to represent a given waveform by a group of tones. In [8], the signal space is partitioned into time/frequency cells, each cell is assigned to one of the available tone frequencies and the total of all cells in the partitioned signal space form an MT-MFSK signal. Another version of MT-MFSK modulation is proposed in [9]. The implementation of this modulation/coding scheme is based on the balanced incomplete block design (BIB-design) from combinatorial theory [13]–[15]. This modulation/coding scheme is an arrangement of v distinct tones into b signals such that each signal contains exactly w distinct tones, each tone occurs in exactly r different signals, and every pair of distinct tones occurs together in exactly one signal. Therefore, the selected tones that are used to represent a signal create implicit diversity, which is a desirable feature when transmitting over a multipath fading channels. Besides, MT-MFSK has the merit of lower complexity, bandwidth, and power efficiency.

Manuscript received March 25, 2004; revised February 10, 2005.

The author is with the Department of Electrical Engineering, Jordan University of Science and Technology, Irbid 22110, Jordan (e-mail: ghareeb@just.edu.jo).

Digital Object Identifier 10.1109/JSAC.2005.853877

TABLE I
ADMISSIBLE VALUES OF v FOR $w = 3$, 4, AND 5, REQUIRED TO REPRESENT $M = 2^{k_s}$ WAVEFORMS FOR THE MT-MFSK MODULATION-BASED $S(v, b, r, w)$, AND A COMPARISONS BETWEEN THESE VALUES TO THOSE REQUIRED BY THE CONVENTIONAL MFSK MODULATION. IN THIS TABLE, l_N AND l_I ARE THE NUMBER OF NONINTERSECTING AND INTERSECTING WAVEFORMS FOR EACH v

–	$S(v,b,r,3)$				$S(v,b,r,4)$				$S(v,b,r,5)$				MFSK
k_s	v	b	l_N	l_I	v	b	l_N	l_I	v	b	l_N	l_I	M
1	7	7	0	6	13	13	0	12	21	21	0	20	2
2	7	7	0	6	13	13	0	12	21	21	0	20	4
3	9	12	2	9	13	13	0	12	21	21	0	20	8
4	13	26	10	15	16	20	3	16	21	21	0	20	16
5	15	35	16	18	25	50	21	28	41	82	36	45	32
6	21	70	42	27	37	111	66	44	41	82	36	45	64
7	31	155	112	42	40	130	81	48	61	183	112	70	128
8	43	301	240	60	61	305	228	76	81	324	228	95	256
9	57	532	450	81	85	595	486	108	105	546	420	125	512
10	79	1027	912	114	112	1036	891	144	145	1044	868	175	1024

However, by combining the implicit diversity created by the MT-MFSK modulation and the diversity reception introduced by employing multiple receiving antennas at the receiver, MT-MFSK system can provide the communication system by a multiplicative diversity. In this paper, MT-MFSK system based on BIB-design with diversity reception is considered. The Performance of this system with noncoherent postdetection SLC and arbitrary correlated Nakagami channels is analyzed, where the effects of diversity, fading severity parameter, and arbitrarily values of correlation between the diversity channels are considered.

This paper is organized as follows. Section II presents a background, mathematical modeling, and system description of MT-MFSK based on BIB-design. Section III presents the performance analysis of the conditional error probability. The performance analysis of the average error probability in arbitrarily correlated and unbalanced Nakagami-m fading channels with diversity reception is evaluated in Section IV. Numerical results and comparisons are given in Section V. Finally, conclusions are drawn in Section VI.

II. SYSTEM MODEL

A. MT-MFSK Modulation

The MT-MFSK modulation is an arrangement of v orthogonal tones into b waveforms, where each waveform contains w distinct tones. Every single tone in a waveform can be used in the transmission of r different waveforms, and every pair of tones occurs in λ waveforms. Such an arrangement, if it exists, is called a MT-MFSK based on BIB-design modulation, with parameters (v, b, r, w, λ). The parameters v, b, r, w, and λ of a BIB-design satisfy the relations $bw = vr$ and $\lambda(v-1) = r(w-1)$ [13]–[15], and for a given v, w, λ the parameters r and b must be integers. In this paper, we consider a particular case of BIB-design with $\lambda = 1$. This case is referred to as Steiner system block design and it will be denoted by $S(v, b, r, w)$. For any given waveform in MT-MFSK based on $S(v, b, r, w)$, there is a total of l_N nonintersecting waveforms and a total of l_I intersecting waveforms on a single tone [14]. The number of nonintersecting and intersecting waveforms are related to v and w by $l_N = b-1+w(v-w)/(w-1)$ and $l_I = w(v-w)/(w-1)$ where $b = l_N + l_I + 1$. Table I show the admissible values of v for different w, required to represent $M = 2^{k_s}$ waveforms for the MT-MFSK modulation based on $S(v, b, r, w)$. A comparison between these values to those required by conventional MFSK modulation is illustrated. The numbers of nonintersecting and intersecting waveforms for each v are also included.

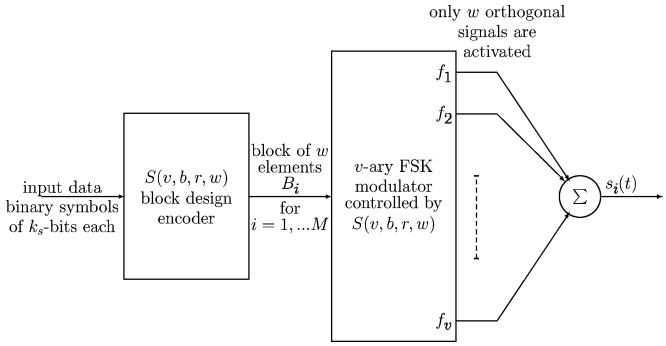

Fig. 1. Block diagram of a MT-MFSK modulator.

A block diagram depicting the modulation process of MT-MFSK signals is shown in Fig. 1. In a symbol interval T_s, every k_s bits of the source stream enter the Steiner system block design $S(v, b, r, w)$ encoder to select a block of w elements. The selected block is then used to activate w tones at the v-ary FSK modulator output. The activated tones are then added to form the MT-MFSK signal. Thus, in MT-MFSK modulation, an $M = 2^{k_s}$ signaling alphabet requires a total of M blocks out of the avaliable b unique blocks to represent the tone assignment to each MT-MFSK waveform. Therefore, to represent the tone assignment to symbols a block $B_i = (a_{i1}, a_{i2}, \ldots, a_{iw})$ for $i = 1, 2, \ldots, M$ containing w tone numbers is associated with each symbol, where $a_{ij} \in \{1, 2, \ldots, v\}$ for $j = 1, 2, \ldots, w$. Hence, the ith signal from a set of $M = 2^{k_s} \leq b$ signals for the MT-MFSK modulated waveform may be represented as

$$s_i(t) = \Re\left\{ \sum_{\substack{k=1 \\ k \in B_i}}^{v} \chi_k(t) e^{j2\pi f_c t} \right\} \quad 0 \leq t \leq T_s, \quad \text{for} \quad i = 1, \ldots, M \quad (1)$$

where $\Re\{\cdot\}$ denotes the real part of the complex-valued quantity in the brackets, f_c is the carrier frequency of $s_i(t)$, and the modulation process $\chi_k(t)$ for $k \in B_i$ represents the equivalent

TABLE II
STEINER SYSTEM BLOCK DESIGN WITH PARAMETERS $v = 13$, $b = 26$, $w = 3$, $r = 6$, AND $\lambda = 1$ REQUIRED TO REPRESENT $M = 16$ WAVEFORMS FOR THE MT-MFSK MODULATION

Message symbols	Steiner system blocks	Message symbols	Steiner system blocks
(0 0 0 0)	B_1 =(1, 3, 9)	(1 1 0 1)	B_{14} =(2, 6, 5)
(0 0 0 1)	B_2 =(2, 4, 10)	(1 1 1 0)	B_{15} =(3, 7, 6)
(0 0 1 0)	B_3 =(3, 5, 11)	(1 1 1 1)	B_{16} =(4, 8, 7)
(0 0 1 1)	B_4 =(4, 6, 12)	(x x x x)	B_{17} =(5, 9, 8)
(0 1 0 0)	B_5 =(5, 7, 13)	(x x x x)	B_{18} =(6, 10, 9)
(0 1 0 1)	B_6 =(6, 8, 1)	(x x x x)	B_{19} =(7, 11, 10)
(0 1 1 0)	B_7 =(7, 9, 2)	(x x x x)	B_{20} =(8, 12, 11)
(0 1 1 1)	B_8 =(8, 10, 3)	(x x x x)	B_{21} =(9, 13, 12)
(1 0 0 0)	B_9 =(9, 11, 4)	(x x x x)	B_{22} =(10, 1, 13)
(1 0 0 1)	B_{10} =(10, 12, 5)	(x x x x)	B_{23} =(11, 2, 1)
(1 0 1 0)	B_{11} =(11, 13, 6)	(x x x x)	B_{24} =(12, 3, 2)
(1 0 1 1)	B_{12} =(12, 1, 7)	(x x x x)	B_{25} =(13, 4, 3)
(1 1 0 0)	B_{13} =(13, 2, 8)	(x x x x)	B_{26} =(1, 5, 4)

low-pass waveform of the kth tone transmitted in the ith signal and it is given by

$$\chi_k(t) = g(t)e^{j2\pi f_k t} \qquad 0 \le t \le T_s, \quad k \in B_i \tag{2}$$

where f_k is one of the orthogonal frequencies chosen according to $f_k = \{(2k - 1 - v)f_d\}$ for $k = 1, 2, \ldots, v$, in which $2f_d = \Delta f$ is the separation between adjacent frequencies. The complex envelope $g(t)$ in (2), determines the spectral characteristics of the signal and it is assumed to be with a constant amplitude $\sqrt{2E_c/T_s}$ and symbol duration T_s, where $E_c = E_s/w$ and E_s is the energy per symbol. The relationship between the symbol duration T_s and the bit duration T_b is given by $T_s = k_s T_b$.

As an example that illustrate the tone assignment of the MT-FSK modulation, we consider a 16-ary message source ($k_s = 4$, $M = 2^{k_s} = 16$) whose output is to be encoded using a Steiner system block design with parameters $v = 13$, $b = 26$, $w = 3$, $r = 6$, and $\lambda = 1$. The 16 possible symbols (messages) and the corresponding blocks B_i for $i = 1, 2, \ldots, 16$ that are required to represent the tone assignment for each symbol are tabulated in Table II. In this example, the number of tones v used to represent the $M = 16$ symbols is equal to 13 and the number of blocks that can be constructed from these tones is $b = 26$, only 16 blocks of the avaliable 26 blocks are used and the remaining blocks B_i for $i = 17, 18, \ldots, 26$ are discarded and not used. Assuming that, the information symbol to be transmitted is (0 0 1 0) and from Table II the corresponding Steiner block is given by $B_3 = (3, 5, 11)$. The elements of B_3 is then used to activate the signals of frequencies f_3, f_5, and f_{11} at the v-ary FSK modulator output, these signal waveforms are then added to form the modulated MT-MFSK signal.

Orthogonality of MT-MFSK frequencies, which are noncoherently detected, requires a minimum frequency separation $\Delta f = 1/T_s$. Consequently, the required channel bandwidth for transmission can be approximated by $W = v\Delta f$. However, the bit rate is given by $R_b = k_s/T_s$. Hence, for noncoherent MT-MFSK, the bandwidth efficiency is given by $\eta_{\mathrm{MT-MFSK}} = k_s/v$. It is well known that for noncoherent MFSK, the bandwidth efficiency is given by $\eta_{\mathrm{MFSK}} = k_s/M$. By the aid of Table I, it clearly appears that, the bandwidth efficiency of MT-MFSK system is greater than that of MFSK system when $k_s > 3$.

B. System Diversity Structure

Consider a diversity reception system, in which the modulated signal is transmitted over a mobile radio fading channel with correlated and unbalanced diversity branches. The equivalent low-pass received signal for the L channels may be expressed as

$$r_l(t) = \sum_{\substack{k=1 \\ k \in B_i}}^{v} \alpha_{l,k} e^{-j\phi_{l,k}} \chi_k(t) + z_{l,k}(t) \quad \text{for } k \in B_i \text{ and } l = 1, 2, \ldots, L \tag{3}$$

where $\alpha_{l,k}$ and $\phi_{l,k}$ are the attenuation factor and phase shift of the channel over the lth path affecting the kth tone of symbol i, respectively, and $z_{l,k}(t)$ represents the additive white Gaussian noise process associated with the kth tone of the ith symbol over the lth channel and it is assumed to be with a zero mean and a one-sided power spectral density N_0. The noise processes $z_{l,k}(t)$ for $k = 1, 2, \ldots, v$ and $l = 1, 2, \ldots, L$ are assumed to be identically distributed and mutually statistically independent. In (3), it is assumed that the separation between successive tones equals or exceeds the coherence bandwidth of the channel.

It is assumed that the diversity branches with the parameters $\alpha_{l,k}e^{-j\phi_{l,k}}$ for $k \in B_i$ and $l = 1, 2, \ldots, L$ are arbitrarily correlated and unbalanced, and each branch is assumed to be frequency nonselective and slowly fading with Nakagami-m-distributed envelope statistics. Therefore, the path gain $\alpha_{l,k}$ is considered to follow a Nakagami-m distribution with a probability density function (pdf)

$$p_{\alpha_{l,k}}(\alpha_{l,k}) = \frac{2}{\Gamma(m_{l,k})} \left(\frac{m_{l,k}}{\Omega_{l,k}}\right)^{m_{l,k}} \alpha_{l,k}^{2m_{l,k}-1} e^{-\frac{m_{l,k}\alpha_{l,k}^2}{\Omega_{l,k}}}, \quad \alpha_{l,k} \ge 0 \tag{4}$$

where $\Gamma(u)$ denoting the Gamma function of u, $\Omega_{l,k} = \mathcal{E}[\alpha_{l,k}^2]$, the operator $\mathcal{E}\{\ \}$ denotes statistical expectation, and $m_{l,k}$ is the fading severity parameter defined as $m_{l,k} = \Omega_{l,k}^2/\mathcal{E}[(\alpha_{l,k}^2 - \Omega_{l,k})^2]$ for $m_{l,k} \ge 1/2$. Note that we have a one-sided Gaussian fading model when $m_{l,k} = 1/2$, and a Rayleigh-fading model when $m_{l,k} = 1$. The values of $m_{l,k}$ between 1/2 and 1 correspond to deeper fading than the Rayleigh fading. Less severe fading is associated with larger values of the fading figure $m_{l,k}$. As $m_{l,k}$ approaches infinity, the fading statistics correspond to nonfading conditions. Furthermore, Nakagami-m distribution can approximate Rician and log-normal fading distributions under certain conditions. The instantaneous signal-to-noise ratio (SNR) per branch $\rho_{c,lk} = \alpha_{l,k}^2 E_c/N_0$ for $l = 1, 2, \ldots, L$, $k \in B_i$ has a Gamma pdf given by

$$p_{\rho_{c,lk}}(\rho_{c,lk}) = \frac{1}{\Gamma(m_{l,k})} \left(\frac{m_{l,k}}{\overline{\rho}_{c,lk}}\right)^{m_{l,k}} \rho_{c,lk}^{m_{l,k}-1} \times \exp\left(-\frac{m_{l,k}}{\overline{\rho}_{c,lk}}\rho_{c,lk}\right), \quad \rho_{c,lk} \ge 0 \tag{5}$$

where $\overline{\rho}_{c,lk} = \mathcal{E}[\alpha_{l,k}^2]E_c/N_0$ is the average SNR for the lth channel.

C. Correlated Nakagami Channels

We are interested in diversity reception systems with post-detection SLC that combine L branches, with joint correlated

Nakagami-m distribution, which are not necessarily have the same power, or even are identical. In a diversity system that combines L branches, the probability of a bit error depends on the instantaneous SNR at the combiner output. The ith information symbol in MT-MFSK modulation is transmitted on w tones selected from the corresponding block B_i, and each tone in the modulated signal is transmitted over a multipath fading channel with L diversity branches. Therefore, the instantaneous SNR at the combiner output for the kth tone is given by $\sum_{l=1}^{L}\rho_{c,lk}$ for $k \in B_i$, and the instantaneous SNR per symbol may be expressed as

$$\rho_s = \frac{E_c}{N_0}\sum_{\substack{k=1\\k\in B_i}}^{v}\sum_{l=1}^{L}\alpha_{l,k}^2 = \sum_{\substack{k=1\\k\in B_i}}^{v}\sum_{l=1}^{L}\rho_{c,lk}. \tag{6}$$

It is well known that the instantaneous SNR per branch $\rho_{c,lk}$ of parameter $m_{l,k}$ can be considered as the sum of squares of $2m_{l,k}$ independent Gaussian random variables [16]. Let $\mathbf{X}_{lk}$ for $l = 1,2,\ldots,L$ and $k \in B_i$ be $2m_{l,k}$-dimensional column vectors defined by

$$\mathbf{X}_{lk} = [x_{lk,1}, x_{lk,2}, \ldots, x_{lk,2m_l}]^T$$

with $x_{lk,n}$ composed of the nth components of the $\mathbf{X}_{lk}$ and $[\,]^T$ denotes the transpose operator. The components $x_{lk,n}$ for $n = 1,2,\ldots,2m_{l,k}$ are assumed to be statistically independent and identically distributed Gaussian random variables with mean zero and variance $\sigma_{lk,n}^2 = \overline{\rho}_{c,lk}/(2m_{l,k}) = \epsilon_{lk}^2$. Therefore, $\rho_{c,lk}$ may be represented by

$$\rho_{c,lk} = \mathbf{X}_{lk}^T\mathbf{X}_{lk} = \sum_{n=1}^{2m_{l,k}} x_{lk,n}^2 \tag{7}$$

and (6) can be written as

$$\rho_s = \sum_{\substack{k=1\\k\in B_i}}^{v}\sum_{l=1}^{L}\rho_{c,lk} = \sum_{\substack{k=1\\k\in B_i}}^{v}\sum_{l=1}^{L}\mathbf{X}_{lk}^T\mathbf{X}_{lk} = \mathbf{X}^T\mathbf{X} \tag{8}$$

where $\mathbf{X}$ is a $\sum_{k=1}^{v}\sum_{l=1}^{L}2m_{l,k}$ for $k \in B_i = \{k_1,k_2,\ldots,k_w\}$ dimensional column vector defined by

$$\mathbf{X} = \left[\mathbf{X}_{1k_1}^T, \mathbf{X}_{2k_1}^T, \ldots, \mathbf{X}_{Lk_1}^T, \ldots, \mathbf{X}_{1k_w}^T, \mathbf{X}_{2k_w}^T, \ldots, \mathbf{X}_{Lk_w}^T\right]^T.$$

The covariance matrix $\mathbf{\Sigma}$ of $\mathbf{X}$ defined by $\mathbf{\Sigma} = E[(\mathbf{X} - E[\mathbf{X}])(\mathbf{X} - E[\mathbf{X}])^T]$ is the $(\sum_{k=1}^{v}\sum_{l=1}^{L}2m_{l,k}) \times (\sum_{k=1}^{v}\sum_{l=1}^{L}2m_{l,k})$ matrix and since $\mathbf{X}$ is with zero mean, $\mathbf{\Sigma}$ can be written as (9) shown at the bottom of the page, where

$$\begin{aligned}\mathbf{\Sigma}_{ik_m,jk_n} &= E\left[\mathbf{X}_{ik_m}\mathbf{X}_{jk_n}^T\right]\\ &= \begin{pmatrix} \sigma_{1,1}^{(ik_m,jk_n)} & \sigma_{1,2}^{(ik_m,jk_n)} & \cdots & \sigma_{1,2m_{j,k_n}}^{(ik_m,jk_n)}\\ \sigma_{2,1}^{(ik_m,jk_n)} & \sigma_{2,2}^{(ik_m,jk_n)} & \cdots & \sigma_{2,2m_{j,k_n}}^{(ik_m,jk_n)}\\ \vdots & \vdots & \ddots & \vdots\\ \sigma_{2m_{i,k_m},1}^{(ik_m,jk_n)} & \sigma_{2m_{i,k_m},2}^{(ik_m,jk_n)} & \cdots & \sigma_{2m_{i,k_m},2m_{j,k_n}}^{(ik_m,jk_n)}\end{pmatrix}\end{aligned} \tag{10}$$

and the element $\sigma_{r,z}^{(ik_m,jk_n)} = E[x_{ik_m,r}x_{jk_n,z}] = c_{ik_m,jk_n}\epsilon_{ik_m}\epsilon_{jk_n}$ is the covariance of the random variables $x_{ik_m,r}$ and $x_{jk_n,z}$, with c_{ik_m,jk_n} is the normalized covariance or correlation coefficient of $x_{ik_m,r}$ and $x_{jk_n,z}$. Without loss of generality one can assume that

$$\begin{aligned}\sigma_{r,z}^{(ik_m,jk_n)} &= E\left[x_{ik_m,r}x_{jk_n,z}\right]\\ &= \begin{cases} c_{ik_m,jk_n}\epsilon_{ik_m}\epsilon_{jk_n}, & r = z\\ 0, & \text{otherwise}\end{cases}.\end{aligned} \tag{11}$$

The covariance of ρ_{c,ik_m} and ρ_{c,jk_n} is given by

$$\begin{aligned}\mathrm{Cov}\left(\rho_{c,ik_m},\rho_{c,jk_n}\right) &= E\left[\left(\rho_{c,ik_m} - \overline{\rho}_{c,ik_m}\right)\left(\rho_{c,jk_n} - \overline{\rho}_{c,jk_n}\right)\right]\\ &= \sum_{e=1}^{2m_{i,k_m}}\sum_{t=1}^{2m_{j,k_n}} E\left[x_{ik_m,e}^2x_{jk_n,t}^2\right]\\ &\quad - \overline{\rho}_{c,ik_m}\overline{\rho}_{c,jk_n}.\end{aligned} \tag{12}$$

By using [20, p. 258, eq. (7.61)], the first term of (12) may be evaluated as

$$\begin{aligned}&\sum_{e=1}^{2m_{i,k_m}}\sum_{t=1}^{2m_{j,k_n}} E\left[x_{ik_m,e}^2x_{jk_n,t}^2\right]\\ &\quad= \sum_{e=1}^{2m_{i,k_m}}\sum_{t=1}^{2m_{j,k_n}} E\left[x_{ik_m,e}^2\right]E\left[x_{jk_n,t}^2\right]\\ &\qquad+ 2\sum_{e=1}^{2m_{i,k_m}}\sum_{t=1}^{2m_{j,k_n}}\left(E\left[x_{ik_m,e}x_{jk_n,t}\right]\right)^2\\ &\quad= \overline{\rho}_{c,ik_m}\overline{\rho}_{c,jk_n} + 4\min\left(m_{i,k_m},m_{j,k_n}\right)c_{ik_m,jk_n}^2\epsilon_{ik_m}^2\epsilon_{jk_n}^2\end{aligned} \tag{13}$$

then

$$\mathrm{Cov}\left(\rho_{c,ik_m},\rho_{c,jk_n}\right) = 4\min\left(m_{i,k_m},m_{j,k_n}\right)c_{ik_m,jk_n}^2\epsilon_{ik_m}^2\epsilon_{jk_n}^2 \tag{14}$$

$$\mathbf{\Sigma} = E[\mathbf{X}\mathbf{X}^T] = \begin{pmatrix} \mathbf{\Sigma}_{1k_1,1k_1} & \mathbf{\Sigma}_{1k_1,2k_1} & \cdots & \mathbf{\Sigma}_{1k_1,Lk_1} & \cdots & \mathbf{\Sigma}_{1k_1,1k_w} & \mathbf{\Sigma}_{1k_1,2k_w} & \cdots & \mathbf{\Sigma}_{1k_1,Lk_w}\\ \mathbf{\Sigma}_{2k_1,1k_1} & \mathbf{\Sigma}_{2k_1,2k_1} & \cdots & \mathbf{\Sigma}_{2k_1,Lk_1} & \cdots & \mathbf{\Sigma}_{2k_1,1k_w} & \mathbf{\Sigma}_{2k_1,2k_w} & \cdots & \mathbf{\Sigma}_{2k_1,Lk_w}\\ \vdots & \vdots & \ddots & \vdots & \vdots & \vdots & \vdots & \ddots & \\ \mathbf{\Sigma}_{Lk_1,1k_1} & \mathbf{\Sigma}_{Lk_1,2k_1} & \cdots & \mathbf{\Sigma}_{Lk_1,Lk_1} & \cdots & \mathbf{\Sigma}_{Lk_1,1k_w} & \mathbf{\Sigma}_{Lk_1,2k_w} & \cdots & \mathbf{\Sigma}_{Lk_1,Lk_w}\\ \vdots & \vdots & \cdots & \vdots & \ddots & \vdots & \vdots & \cdots & \vdots\\ \mathbf{\Sigma}_{1k_w,1k_1} & \mathbf{\Sigma}_{1k_w,2k_1} & \cdots & \mathbf{\Sigma}_{1k_w,Lk_1} & \cdots & \mathbf{\Sigma}_{1k_w,1k_w} & \mathbf{\Sigma}_{1k_w,2k_w} & \cdots & \mathbf{\Sigma}_{1k_w,Lk_w}\\ \mathbf{\Sigma}_{2k_w,1k_1} & \mathbf{\Sigma}_{2k_w,2k_1} & \cdots & \mathbf{\Sigma}_{2k_w,Lk_1} & \cdots & \mathbf{\Sigma}_{2k_w,1k_w} & \mathbf{\Sigma}_{2k_w,2k_w} & \cdots & \mathbf{\Sigma}_{2k_w,Lk_w}\\ \vdots & \vdots & \ddots & \vdots & \vdots & \vdots & \vdots & \ddots & \\ \mathbf{\Sigma}_{Lk_w,1k_1} & \mathbf{\Sigma}_{Lk_w,2k_1} & \cdots & \mathbf{\Sigma}_{Lk_w,Lk_1} & \cdots & \mathbf{\Sigma}_{Lk_w,1k_w} & \mathbf{\Sigma}_{Lk_w,2k_w} & \cdots & \mathbf{\Sigma}_{Lk_w,Lk_w}\end{pmatrix} \tag{9}$$

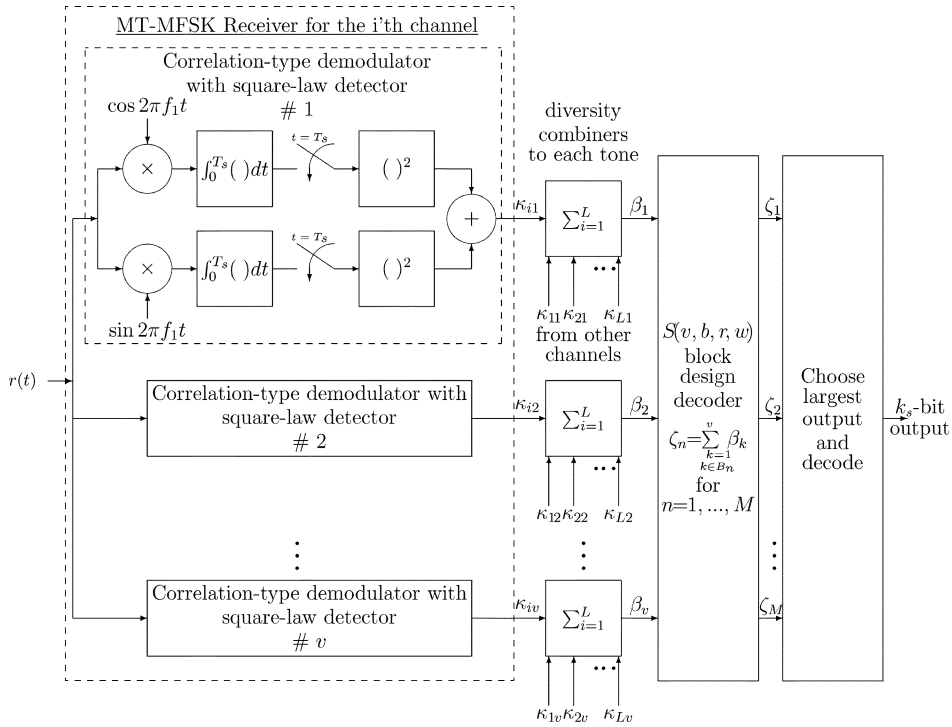

Fig. 2. Block diagram of a noncoherent MT-MFSK diversity receiver and combiner with $S(v, b, r, w)$ decoder.

substituting the value of c_{ik_m,jk_n} given in (14) into (11), we obtain

$$\sigma_{r,z}^{(ik_m,jk_n)} = E\left[x_{ik_m,r}x_{jk_n,z}\right] = \begin{cases} \sqrt{\frac{\mathrm{Cov}(\rho_{c,ik_m},\rho_{c,jk_n})}{4\min(m_{i,k_m},m_{j,k_n})}}, & r = z \\ 0, & \text{otherwise} \end{cases}. \quad (15)$$

By using the Karhunen–Loeve expansion of vector $\mathbf{X}$, we obtain

$$\mathbf{X} = \sum_{n=1}^{N} \sqrt{\lambda_n} Z_n \mathbf{Q}_n \quad (16)$$

where $N = \sum_{k=1}^{v}\sum_{l=1}^{L} 2m_{l,k}$ for $k \in B_i = \{k_1, k_2, \ldots, k_w\}$, λ_n for $n = 1, 2, \ldots, N$ are the eigenvalues of the covariance matrix $\mathbf{\Sigma}$, $\mathbf{Q}_n$ for $n = 1, 2, \ldots, N$ are the orthonormal eigenvectors corresponding to λ_n for $n = 1, 2, \ldots, N$, and Z_n for $n = 1, 2, \ldots, N$ are independent zero mean and unity variance Gaussian random variables. Therefore, the instantaneous SNR at the combiner output ρ_s, may be written as

$$\rho_s = \sum_{n=1}^{N} \lambda_n Z_n^2. \quad (17)$$

The characteristic function of ρ_s is defined as

$$\Phi_{\rho_s}(jt) = E\left[\exp(jt\rho_s)\right] = E\left[\exp\left(jt\sum_{n=1}^{N}\lambda_n Z_n^2\right)\right] \quad (18)$$

since Z_n for $n = 1, 2, \ldots, N$ are independent random variables, (18) can be expressed as

$$\Phi_{\rho_s}(jt) = \prod_{n=1}^{N} E\left[\exp\left(jt\lambda_n Z_n^2\right)\right] \quad (19)$$

but Z_n^2 has a chi-square distribution with a characteristic function given by

$$E\left[e^{jZ_n^2 t}\right] = \frac{1}{(1-j2t)^{\frac{1}{2}}}. \quad (20)$$

Consequently, the characteristic function of ρ_s is

$$\Phi_{\rho_s}(jt) = \frac{1}{\prod_{n=1}^{N}(1-j2\lambda_n t)^{\frac{1}{2}}}. \quad (21)$$

For a special case when all diversity branches have the same fading severity parameter, similar result were obtained by [21].

III. Conditional Error Probability

A. Diversity Combining and Decision Variable

For the ith channel, a block diagram of a noncoherent MT-MFSK diversity receiver and combiner with $S(v, b, r, w)$ decoder is shown in Fig. 2. The receiver for each channel consists of v branches; each branch is tuned to one of the baseband frequencies, say f_j for $j = 1, 2, \ldots, v$. The correlator outputs are sampled every symbol duration T_s and followed by a square-law detector. The sampled values κ_{ij} for $i = 1, 2, \ldots, L$ and $j = 1, 2, \ldots, v$ are linearly combined for each symbol to form the branch variables β_j for $j = 1, 2, \ldots, v$. These variables are then processed by the $S(v, b, r, w)$ decoder to form the decision variables ζ_n for $n = 1, 2, \ldots, M$. These decision variables are then compared and the decision on the transmitted symbol is made by taking the largest ζ_n.

Assume that, the signal $s_i(t)$ with w tones, $\{f_k, k \in B_i : k = 1, 2, \ldots, v\}$ is transmitted. Then the conditional probability of a correct decision is

$$P_c(\rho_s) = \Pr\left(\zeta_i = \max_{n=1,\ldots,M}[\zeta_n]\right). \quad (22)$$

According to $S(v,b,r,w)$, the decision variable ζ_n may be expressed as

$$\zeta_n = \sum_{\substack{k=1 \\ k\in B_n}}^{v} \beta_k \quad \text{for } n = 1,2,\ldots,M \tag{23}$$

and the decision sample β_k for $k \in B_n$ is given by

$$\beta_k = \sum_{l=1}^{L} \kappa_{lk} \quad \text{for} \quad k \in B_n \quad \text{and} \quad n = 1,2,\ldots,M. \tag{24}$$

The sampled values κ_{lk} for $l = 1,2,\ldots,L$, $k \in B_n$ and $n = 1,2,\ldots,M$, that include the transmitted signal components can be written as

$$\kappa_{lk} = \left|2E_c\alpha_{l,k}e^{-j\phi_{l,k}} + N_{l,k}\right|^2 \quad \text{for } l = 1,2,\ldots,L, \text{ and } k \in B_i \tag{25}$$

and due to tones orthogonality; the other correlator and square-law detector outputs are

$$\kappa_{lk} = |N_{l,k}|^2 \quad \text{for } l = 1,2,\ldots,L \text{ and } k \notin B_i \tag{26}$$

where E_c is the average symbol energy per branch and $N_{l,k}$ for $l = 1,2,\ldots,L$, and $k = 1,2,\ldots,v$ are the received noise components at the correlator outputs and they are mutually statistically independent Gaussian random variables with zero means.

The decision variables ζ_n for $n \neq i$ can be divided into two sets relative to ζ_i. The first set (the nonintersecting set) consists of l_N elements $\zeta'_1,\zeta'_2,\ldots,\zeta'_{l_N}$. In this set, there is no decision sample β_k for $k \notin B_i$ in common to ζ_i. The second set (the intersecting set) consists of l_I elements, $\zeta''_1,\zeta''_2,\ldots,\zeta''_{l_I}$. This set, has only one decision sample β_k for $k \notin B_i$ in common to ζ_i. The conditional probability of a correct decision for a given set of channel gains $\{\alpha_{l,k}, l = 1,2,\ldots,L \text{ and } k = 1,2,\ldots,v\}$ in (22) may be expressed as

$$P_c(\rho_s) = \Pr\Big(\zeta_i > \zeta'_1 \bigcap \zeta_i > \zeta'_2 \bigcap \cdots \bigcap \zeta_i > \zeta'_{l_N} \bigcap \zeta_i > \zeta''_1 \bigcap \zeta_i > \zeta''_2 \bigcap \cdots \bigcap \zeta_i > \zeta''_{l_I} | \alpha\Big). \tag{27}$$

Therefore, the conditional probability of symbol error, $P_E(\rho_s) = 1 - P_c(\rho_s)$, can be written in the form of

$$P_E(\rho_s) = \Pr\left\{\left(\bigcup_{k=1}^{l_N}(\zeta_i < \zeta'_k|\alpha)\right)\bigcup\left(\bigcup_{k=1}^{l_I}(\zeta_i < \zeta''_k|\alpha)\right)\right\}. \tag{28}$$

The decision variables ζ''_k for $k = 1,\ldots,l_I$ are all statistically dependent on ζ_i and/or ζ'_k for $k = 1,\ldots,l_N$ due to the nature of the BIB-design structure. By noting that, the probability of a finite union of events can be bounded above by the sum of the probabilities of constituent events, a union bound on the conditional probability of error can be obtained, and it is given by

$$P_E(\rho_s) \leq \sum_{k=1}^{l_N}\Pr(\zeta_i < \zeta'_k|\alpha) + \sum_{k=1}^{l_I}\Pr(\zeta_i < \zeta''_k|\alpha). \tag{29}$$

Furthermore, the probabilities $\Pr(\zeta_i < \zeta'_k|\alpha)$ for $k = 1,2,\ldots,l_N$ are equal and the probabilities $\Pr(\zeta_i < \zeta''_k|\alpha)$ for $k = 1,2,\ldots,l_I$ are also equal. Hence, (29) reduces to

$$P_E(\rho_s) \leq l_N\Pr(\zeta_i < \zeta'_k|\alpha) + l_I\Pr(\zeta_i < \zeta''_k|\alpha). \tag{30}$$

Computation of the upper bound for the conditional probability of symbol error in (30) requires $\Pr(\zeta_i < \zeta'_k|\alpha)$ and $\Pr(\zeta_i < \zeta''_k|\alpha)$. The random variables ζ_i and ζ'_k for $k = 1,2,\ldots,l_N$ are statistically independent. Therefore, the joint pdf required to obtain $\Pr(\zeta_i < \zeta'_k|\alpha)$ can be obtained in a straightforward manner. On the other hand, the random variables ζ_i and ζ''_k for $k = 1,2,\ldots,l_I$ are statistically dependent, in this case, evaluation of the second term of (30) cannot be obtained directly and requires formulation of an alternative decision variable.

B. Analysis of $\Pr(\zeta_i < \zeta'_k|\alpha)$

Let us assume that $s_i(t)$ with w tones, $\{f_k, k \in B_i : k = 1,2,\ldots,v\}$, was transmitted. We begin with the conditional statistics of the sampled output κ_{lk} for a given set of channel gains $\{\alpha_{l,k}, l = 1,2,\ldots,L \text{ and } k = 1,2,\ldots,v\}$. Since the noise components $\{N_{l,k}\}$ are all mutually statistically independent Gaussian distributed with zero mean for all l and k, it follows [17, p. 42] that the conditional pdf of κ_{lk} is a chi-square with two degrees of freedom and has a characteristic function given by

$$\Phi_{\kappa_{lk}}(jt|\alpha) = \begin{cases} \frac{1}{(1-jt2\sigma^2_{lk})}\exp\left(jt\frac{\mu^2_{lk}}{1-jt2\sigma^2_{lk}}\right), & k \in B_i \\ \frac{1}{(1-jt2\sigma^2_{lk})}, & k \notin B_i \end{cases} \tag{31}$$

where $\sigma^2_{lk} = 2E_cN_0$ and $\mu_{lk} = 2E_c\alpha_{l,k}$.

It is assumed that the frequencies are orthogonal and the L channels are statistically independent, then the output samples κ_{lk} for $k = 1,2,\ldots,v$ are statistically independent and, hence, β_k for $k = 1,2,\ldots,v$ are also statistically independent. Therefore, the characteristic function of β_k can be found to be

$$\Phi_{\beta_k}(jt|\alpha) = \begin{cases} \prod_{l=1}^{L}\frac{1}{(1-jt2\sigma^2_{lk})}\exp\left(jt\frac{\mu^2_{lk}}{1-jt2\sigma^2_{lk}}\right), & k \in B_i \\ \prod_{l=1}^{L}\frac{1}{(1-jt2\sigma^2_{lk})}, & k \notin B_i \end{cases} \tag{32}$$

and hence, the characteristic function of ζ_n for the nonintersecting set is given by

$$\Phi_{\zeta_n}(jt|\alpha) = \begin{cases} \prod_{\substack{k=1 \\ k\in B_i}}^{v}\prod_{l=1}^{L}\frac{1}{(1-jt2\sigma^2_{lk})}\exp\left(jt\frac{\mu^2_{lk}}{1-jt2\sigma^2_{lk}}\right), & k \in B_i \\ \prod_{\substack{k=1 \\ k\notin B_i}}^{v}\prod_{l=1}^{L}\frac{1}{(1-jt2\sigma^2_{lk})}, & k \notin B_i \end{cases}. \tag{33}$$

Since $\sigma^2_{lk} = 2E_cN_0 = \sigma^2$ is a constant for all l and k, $\mu_{lk} = 2E_c\alpha_{l,k}$ and the block B_n for $n = 1,2,\ldots,M$ contains w elements, (33) can be expressed in the form

$$\Phi_{\zeta_n}(jt|\alpha) = \begin{cases} \frac{1}{(1-jt2\sigma^2)^{wL}}\exp\left(jt\sum_{\substack{k=1 \\ k\in B_i}}^{v}\sum_{l=1}^{L}\frac{\mu^2_{lk}}{1-jt2\sigma^2}\right), & k \in B_i \\ \frac{1}{(1-jt2\sigma^2)^{wL}}, & k \notin B_i \end{cases}. \tag{34}$$

Now, the pdf of ζ_n for the nonintersecting set (inverse transform of $\Phi_{\zeta_n}(jt|\alpha)$) becomes (35), as shown at the bottom of the page, where μ^2 is the noncentrality parameter, which is equal to

$$\mu^2 = \sum_{\substack{k=1\\k\in B_i}}^{v}\sum_{l=1}^{L}\mu_{l,k}^2 = \sum_{\substack{k=1\\k\in B_i}}^{v}\sum_{l=1}^{L}(2E_c\alpha_{l,k})^2 \tag{36}$$

and $I_k(x)$ is the kth order modified Bessel function of the first kind, which can be defined as

$$I_k(x)=\sum_{n=0}^{\infty}\frac{\left(\frac{x}{2}\right)^{k+2n}}{n!\Gamma(k+n+1)}=\frac{1}{\pi}\int_0^{\pi}\exp(x\cos\theta)\cos(k\theta)d\theta. \tag{37}$$

Having obtained the pdf of ζ_n for the nonintersecting set, it is well known that the probability of the first term given in (30) is given by

$$\Pr(\zeta_i<\zeta_k'|\alpha)=1-\int_0^{\infty}p_{\zeta_i}(\zeta|\alpha)\left[\int_0^{\zeta}p_{\zeta_k}(x|\alpha)dx\right]d\zeta \quad \text{for } k\neq i. \tag{38}$$

The integral in the square brackets can be evaluated by using [19, p. 310], and $\Pr(\zeta_i<\zeta_k'|\alpha)$ may be expressed as

$$\Pr(\zeta_i<\zeta_k'|\alpha)=1-\int_0^{\infty}p_{\zeta_i}(\zeta|\alpha)\times\left[1-e^{-\frac{\zeta}{4E_cN_0}}\sum_{k=0}^{wL-1}\frac{1}{k!}\left(\frac{\zeta}{4E_cN_0}\right)^k\right]d\zeta. \tag{39}$$

By substituting $\nu=\zeta/4E_cN_0$, and taking into consideration the definitions of μ^2 and $p_{\zeta_i}(\zeta|\alpha)$, the above probability can be written as

$$\Pr(\zeta_i<\zeta_k'|\alpha)=\sum_{k=0}^{wL-1}\frac{1}{k!}\frac{e^{-\rho_s}}{\rho_s^{\frac{(wL-1)}{2}}}\int_0^{\infty}e^{-2\nu}\nu^{\left(\frac{k+(wL-1)}{2}\right)}\times I_{L-1}(2\sqrt{\rho_s\nu})d\nu. \tag{40}$$

The integral in (40) can be evaluated by using [19, p. 716], therefore, the above probability yields to

$$\Pr(\zeta_i<\zeta_k'|\alpha)=\frac{e^{-\rho_s}}{2^{wL}\Gamma(wL)}\sum_{k=0}^{wL-1}\frac{\Gamma(wL+k)}{2^k k!}\times{}_1F_1\left(wL+k;wL;\frac{\rho_s}{2}\right) \tag{41}$$

where

$${}_1F_1(a;b;x)=\frac{\Gamma(b)}{\Gamma(a)}\sum_{k=0}^{\infty}\frac{\Gamma(a+k)x^k}{\Gamma(b+k)k!} \quad b\neq 0,-1,-2,\ldots \tag{42}$$

is the confluent hypergeometric function and ρ_s is the SNR per symbol and it is given by

$$\rho_s=k_s\rho_b=\frac{E_c}{N_0}\sum_{\substack{k=1\\k\in B_i}}^{v}\sum_{l=1}^{L}\alpha_{l,k}^2=\sum_{\substack{k=1\\k\in B_i}}^{v}\sum_{l=1}^{L}\rho_{c,lk} \tag{43}$$

where ρ_b is the SNR per bit and $\rho_{c,lk}$ is the SNR per branch.

C. Analysis of $\Pr(\zeta_i<\zeta_k''|\alpha)$

Now, let us evaluate the probability of the second term given in (30) (i.e., the intersecting set in one decision sample). The probability of this term may be expressed as

$$\begin{aligned}&\Pr(\zeta_i<\zeta_k''|\alpha)\\&\quad=\Pr(\zeta_i-\zeta_k''<0|\alpha)\\&\quad=\Pr\left(\sum_{\substack{k=1\\k\in B_i}}^{v}\beta_k-\sum_{\substack{k=1\\k\in B_n}}^{v}\beta_k<0|\alpha\right)\quad n\neq i.\end{aligned} \tag{44}$$

According to Steiner system block design $S(v,b,r,w)$, the two blocks B_i and B_n cannot have more than one point out of w points in common, therefore, the decision variables ζ_i and ζ_k'', overlap in one decision sample β_k for $k\in B_i$. Without loss of generality, if we assume that ζ_i intersect with ζ_k'' in the decision sample β_e, then (44) may be written as

$$\Pr(\zeta_i<\zeta_k''|\alpha)=\Pr\left(\sum_{\substack{k=1,k\neq e\\k\in B_i}}^{v}\beta_k-\sum_{\substack{k=1,k\neq e\\k\in B_n}}^{v}\beta_k<0|\alpha\right)\ n\neq i. \tag{45}$$

Therefore, the decision samples β_k for $k\in B_i$, $k\neq e$ and β_k for $k\in B_n$, $k\neq e$ are all statistically independent and $\Pr(\zeta_i<\zeta_k''|\alpha)$ can be derived based on the analysis of $\Pr(\zeta_i<\zeta_k'|\alpha)$. According to the analysis of $\Pr(\zeta_i<\zeta_k'|\alpha)$, the $\Pr(\zeta_i<\zeta_k''|\alpha)$ can be obtained by replacing w in (41) by $\overline{w}=w-1$ and the result is given by

$$\Pr(\zeta_i<\zeta_k''|\alpha)=\frac{e^{-\gamma_s}}{2^{\overline{w}L}\Gamma(\overline{w}L)}\sum_{k=0}^{\overline{w}L-1}\frac{\Gamma(\overline{w}L+k)}{2^k k!}\times{}_1F_1\left(\overline{w}L+k;\overline{w}L;\frac{\gamma_s}{2}\right) \tag{46}$$

$$p_{\zeta_n}(\zeta|\alpha)=\begin{cases}\frac{1}{2\sigma^2}\left(\frac{\zeta}{\mu^2}\right)^{\frac{(wL-1)}{2}}\exp\left(-\frac{\mu^2+\zeta}{2\sigma^2}\right)I_{wL-1}\left(\frac{\mu\sqrt{\zeta}}{\sigma^2}\right) & \text{for } \zeta_i,\ \zeta\geq 0.\\ \frac{\zeta^{wL-1}}{(2\sigma^2)^{wL}(wL-1)!}\exp\left(-\frac{\zeta}{2\sigma^2}\right) & \text{for } \zeta_1',\zeta_2',\ldots,\zeta_{l_N}',\ \zeta\geq 0.\end{cases} \tag{35}$$

where

$$\gamma_s = \frac{E_c}{N_0} \sum_{\substack{k=1,k\neq e\\ k\in B_i}}^{v} \sum_{l=1}^{L} \alpha_{l,k}^2 = \sum_{\substack{k=1,k\neq e\\ k\in B_i}}^{v} \sum_{l=1}^{L} \rho_{c,lk}. \quad (47)$$

A union bound on the conditional probability of symbol error for MT-MFSK signals is now obtained by substituting (41) and (46) into (30), which yields

$$\begin{aligned} P_E(\rho_s) \leq\, & l_N \frac{e^{-\rho_s}}{2^{wL}\Gamma(wL)} \sum_{k=0}^{wL-1} \frac{\Gamma(wL+k)}{2^k k!} \\ & \times {}_1F_1\left(wL+k; wL; \frac{\rho_s}{2}\right) + l_I \frac{e^{-\gamma_s}}{2^{\overline{w}L}\Gamma(\overline{w}L)} \\ & \times \sum_{k=0}^{\overline{w}L-1} \frac{\Gamma(\overline{w}L+k)}{2^k k!} {}_1F_1\left(\overline{w}L+k; \overline{w}L; \frac{\gamma_s}{2}\right). \quad (48) \end{aligned}$$

IV. Average Error Probability

An average union bound on the probability of error is evaluated by averaging (48) over the pdf of the output SNR, and the result can be expressed as

$$\begin{aligned} P_E \leq\, & l_N \int_{\rho_s} \Pr\left(\zeta_i < \zeta_k' | \rho_s\right) p_{\rho_s}(\rho_s) d\rho_s \\ & + l_I \int_{\gamma_s} \Pr\left(\zeta_i < \zeta_k'' | \gamma_s\right) p_{\gamma_s}(\gamma_s) d\gamma_s \\ =\, & l_N \Pr\left(\zeta_i < \zeta_k'\right) + l_I \Pr\left(\zeta_i < \zeta_k''\right). \quad (49) \end{aligned}$$

The $\Pr(\zeta_i < \zeta_k')$ is evaluated by averaging (41) over the pdf of the output SNR ρ_s, and the result may be written as

$$\begin{aligned} & \Pr\left(\zeta_i < \zeta_k'\right) \\ & = \int_{\rho_s} \Pr\left(\zeta_i < \zeta_k' | \rho_s\right) p_{\rho_s}(\rho_s) d\rho_s \\ & = \int_{\rho_s=0}^{\infty} \sum_{k=0}^{wL-1} \frac{\Gamma(wL+k)}{2^{(wL+k)} k! \Gamma(wL)} \\ & \quad \times e^{-\rho_s} {}_1F_1\left(wL+k; wL; \frac{\rho_s}{2}\right) p_{\rho_s}(\rho_s) d\rho_s. \quad (50) \end{aligned}$$

By using the definition of the characteristic function (CF) of the instantaneous SNR $\Phi_{\rho_s}(jt)$

$$\Phi_{\rho_s}(jt) = \int_{-\infty}^{\infty} p_{\rho_s}(\rho_s) e^{jt\rho_s} d\rho_s \quad (51)$$

the average probability in (50) can be rewritten as

$$\begin{aligned} \Pr\left(\zeta_i < \zeta_k'\right) = & \int_{\rho_s=0}^{\infty} \sum_{k=0}^{wL-1} \frac{\Gamma(wL+k)}{2^{(wL+k)} k! \Gamma(wL)} e^{-\rho_s} \\ & \times {}_1F_1\left(wL+k; wL; \frac{\rho_s}{2}\right) \left[\frac{1}{2\pi} \int_{-\infty}^{\infty} \Phi_{\rho_s}(jt) e^{-jt\rho_s} dt\right] d\rho_s. \quad (52) \end{aligned}$$

Interchanging the order of integration, we have

$$\begin{aligned} \Pr\left(\zeta_i < \zeta_k'\right) = & \frac{1}{2\pi} \sum_{k=0}^{wL-1} \frac{\Gamma(wL+k)}{2^{(wL+k)} k! \Gamma(wL)} \int_{-\infty}^{\infty} \Phi_{\rho_s}(jt) \\ & \times \left[\int_0^{\infty} e^{-(1+jt)\rho_s} {}_1F_1\left(wL+k; wL; \frac{\rho_s}{2}\right) d\rho_s\right] dt. \quad (53) \end{aligned}$$

The second integral can be evaluated using [19, p. 851] and (53) can be rewritten as

$$\begin{aligned} \Pr\left(\zeta_i < \zeta_k'\right) = & \frac{1}{2\pi} \sum_{k=0}^{wL-1} \frac{\Gamma(wL+k)}{2^{(wL+k)} k! \Gamma(wL)} \int_{-\infty}^{\infty} \frac{\Phi_{\rho_s}(jt)}{1+jt} \\ & \times {}_2F_1\left(wL+k, 1; wL; \frac{1}{2(1+jt)}\right) dt \quad (54) \end{aligned}$$

where ${}_2F_1(a,b;c;x)$ is the Gaussian hypergeometric function defined as

$${}_2F_1(a,b;c;x) = \frac{\Gamma(c)}{\Gamma(a)\Gamma(b)} \sum_{k=0}^{\infty} \frac{\Gamma(a+k)\Gamma(b+k)x^k}{\Gamma(c+k)k!}. \quad (55)$$

It is easy to show that, the real part of the function

$$G(jt) = \frac{\Phi_{\rho_s}(jt)}{1+jt} {}_2F_1\left(wL+k, 1; wL; \frac{1}{2(1+jt)}\right) \quad (56)$$

is an even function of t, and its imaginary part is an odd function of t. Therefore

$$\Pr\left(\zeta_i < \zeta_k'\right) = \frac{1}{\pi} \sum_{k=0}^{wL-1} \frac{\Gamma(wL+k)}{2^{(wL+k)} k! \Gamma(wL)} \int_0^{\infty} \Re\left[G(jt)\right] dt. \quad (57)$$

Now, according to the analysis of $\Pr(\zeta_i < \zeta_k')$, the $\Pr(\zeta_i < \zeta_k'')$ can be obtained by replacing w in (57) by $\overline{w} = w - 1$ and the result my be expressed as

$$\Pr\left(\zeta_i < \zeta_k''\right) = \frac{1}{\pi} \sum_{k=0}^{\overline{w}L-1} \frac{\Gamma(\overline{w}L+k)}{2^{(\overline{w}L+k)} k! \Gamma(\overline{w}L)} \int_0^{\infty} \Re\left[\overline{G}(jt)\right] dt \quad (58)$$

where

$$\overline{G}(jt) = \frac{\Phi_{\gamma_s}(jt)}{1+jt} {}_2F_1\left(\overline{w}L+k, 1; \overline{w}L; \frac{1}{2(1+jt)}\right). \quad (59)$$

An average union bound on the probability of symbol error for MT-MFSK signals is now obtained by substituting (57) and (58) into (49), which yields

$$\begin{aligned} P_E \leq\, & l_N \frac{1}{\pi} \sum_{k=0}^{wL-1} \frac{\Gamma(wL+k)}{2^{(wL+k)} k! \Gamma(wL)} \int_0^{\infty} \Re\left[G(jt)\right] dt \\ & + l_I \frac{1}{\pi} \sum_{k=0}^{\overline{w}L-1} \frac{\Gamma(\overline{w}L+k)}{2^{(\overline{w}L+k)} k! \Gamma(\overline{w}L)} \int_0^{\infty} \Re\left[\overline{G}(jt)\right] dt. \quad (60) \end{aligned}$$

A union bound on the probability of symbol error for the conventional MFSK signals can be obtained by substituting $w = 1$, $l_N = M - 1$, and $l_I = 0$ into (60), which

$$P_E \leq (M-1) \frac{1}{\pi} \sum_{k=0}^{L-1} \frac{\Gamma(L+k)}{2^{(L+k)} k! \Gamma(L)} \int_0^{\infty} \Re\left[G(jt)\right] dt. \quad (61)$$

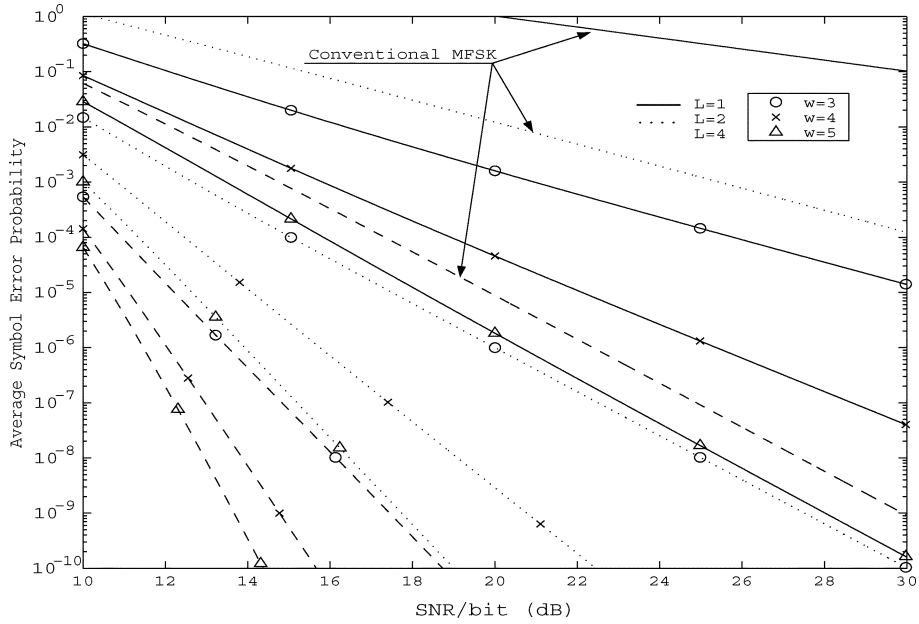

Fig. 3. Average symbol error probability versus average SNR per bit for the conventional MFSK system and different configurations of MT-MFSK system with $w = 3, 4, 5$, $k_s = 10$, $L = 1, 2, 4$, and $m = 1$.

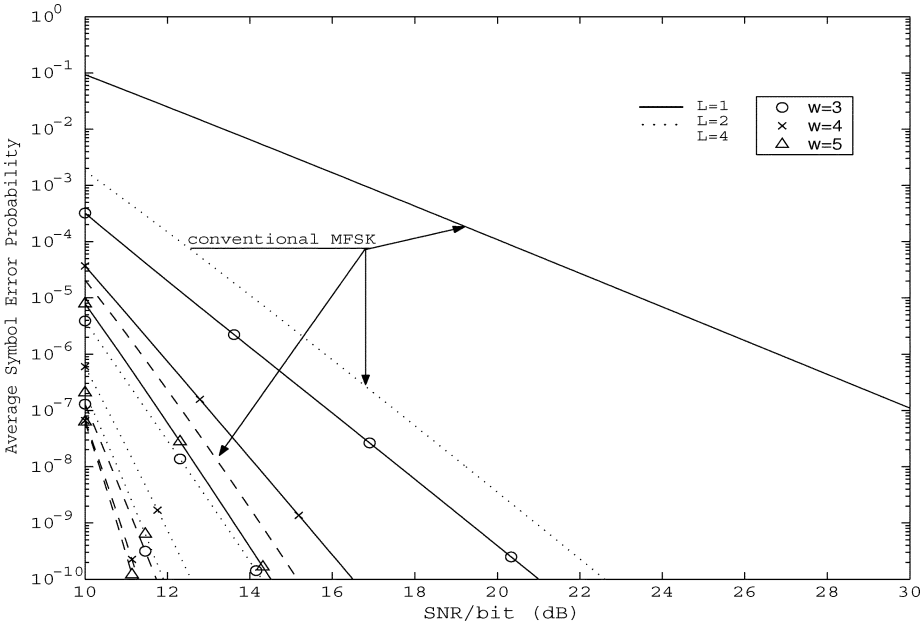

Fig. 4. Average symbol error probability versus average SNR per bit for the conventional MFSK system and different configurations of MT-MFSK system with $w = 3, 4, 5$, $k_s = 10$, $L = 1, 2, 4$, and $m = 3$.

V. Numerical Results

The average union bound on the symbol error probability P_E from (60) versus average SNR per bit $\bar{\rho}_b$, when the diversity channels are mutually statistically independent, has been calculated numerically for different schemes of MT-MFSK system with $w = 3, 4, 5$, $k_s = 10$, $L = 1, 2, 4$, and $m_{l,k} = m = 1, 3$ for all l, k. These data are compared with the symbol error probability of the conventional MFSK system from (61) for $k_s = 10$ and $L = 1, 2, 4$, and the results have been plotted in Figs. 3 and 4. From these curves it is observed that: for all systems, for a given symbol error probability and as the diversity level is increased, significant performance gain is achieved compared with a single diversity level system. Also, for a given symbol error probability and diversity level L, significant performance gain is achieved compared with the conventional MFSK system. More performance gains can be achieved by using different configurations of MT-MFSK system, where, it can be observed that for a given diversity level and as w is increased more power gain can be achieved.

The average symbol error probability as a function of average SNR per bit has been calculated numerically for different configurations of MT-MFSK system with $w = 3, 5$, $L = 2$, and $k_s = 4, 6, 8$, and 10 when the fading severity parameter $m_{l,k} = m = 1, 3$.

These data are compared with the conventional MFSK system for $k_s = 4, 6, 8, 10$ and $L = 2$, and the results are illustrated

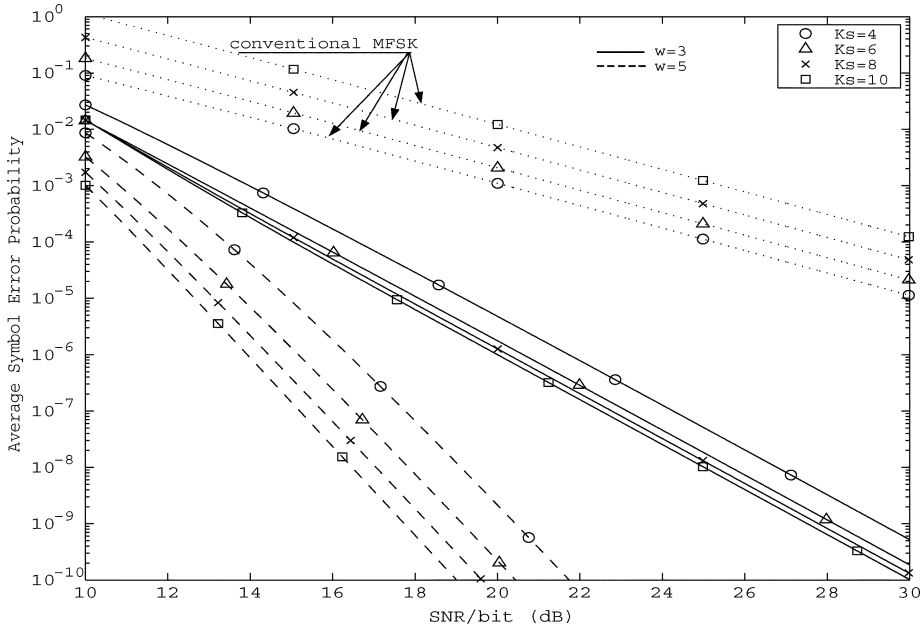

Fig. 5. Average symbol error probability versus average SNR per bit for the conventional MFSK system and different configurations of MT-MFSK system with $w = 3, 5$, $k_s = 4, 6, 8, 10$, $L = 2$, and $m = 1$.

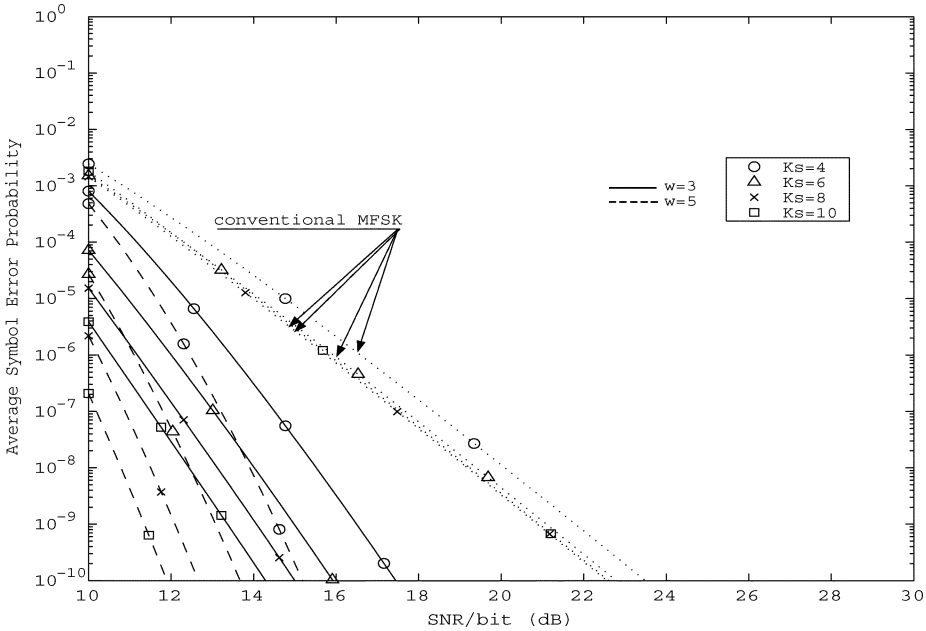

Fig. 6. Average symbol error probability versus average SNR per bit for the conventional MFSK system and different configurations of MT-MFSK system with $w = 3, 5$, $k_s = 4, 6, 8, 10$, $L = 2$, and $m = 3$.

in Figs. 5 and 6. From these figures, it can be observed that as $M = 2^{ks}$ is increased more power gain can be achieved, and the gain in performance with an increase in k_s is relatively small for a given w. Also, significant performance gain is achieved compared with the conventional MFSK system for a given k_s, at a symbol error probability of 10^{-6} MT-MFSK system with $w = 3$, $k_s = 6$, and $m = 1$ has a gain of more than 11 dB for $L = 2$ in average SNR per bit compared with the conventional MFSK with $k_s = 6$ and $L = 2$. More performance gains can be achieved by using other configurations of MT-MFSK systems. For example, at a symbol error probability of 10^{-6}, using MT-MFSK system with $w = 5$ and $k_s = 6$ provides more than 16 dB for $L = 2$ improvement over the conventional MFSK with $k_s = 6$ and $L = 2$. The comparisons of MT-MFSK and the conventional MFSK are made in terms of power efficiency (i.e.,

TABLE III
COMPARISON BETWEEN MT-MFSK AND MFSK, BASED ON THE BANDWIDTH EFFICIENCY R_b/W VERSUS SNR PER BIT $\bar{\rho}_b$ REQUIRED TO ACHIEVE A SYMBOL ERROR PROBABILITY OF 10^{-6} IN NAKAGAMI CHANNEL WITH $m = 1$ AND $L = 2$

–	MT-MFSK, $w = 3$		MT-MFSK, $w = 5$		MFSK	
k_s	R_b/W	$\bar{\rho}_b$	R_b/W	$\bar{\rho}_b$	R_b/W	$\bar{\rho}_b$
4	0.3077	21.8	0.1905	16.4	0.2500	32.5
6	0.2857	20.7	0.1463	15.2	0.0937	32.0
8	0.1861	20.3	0.0988	14.5	0.0313	31.5
10	0.1266	20.0	0.0689	13.9	0.0098	31.2

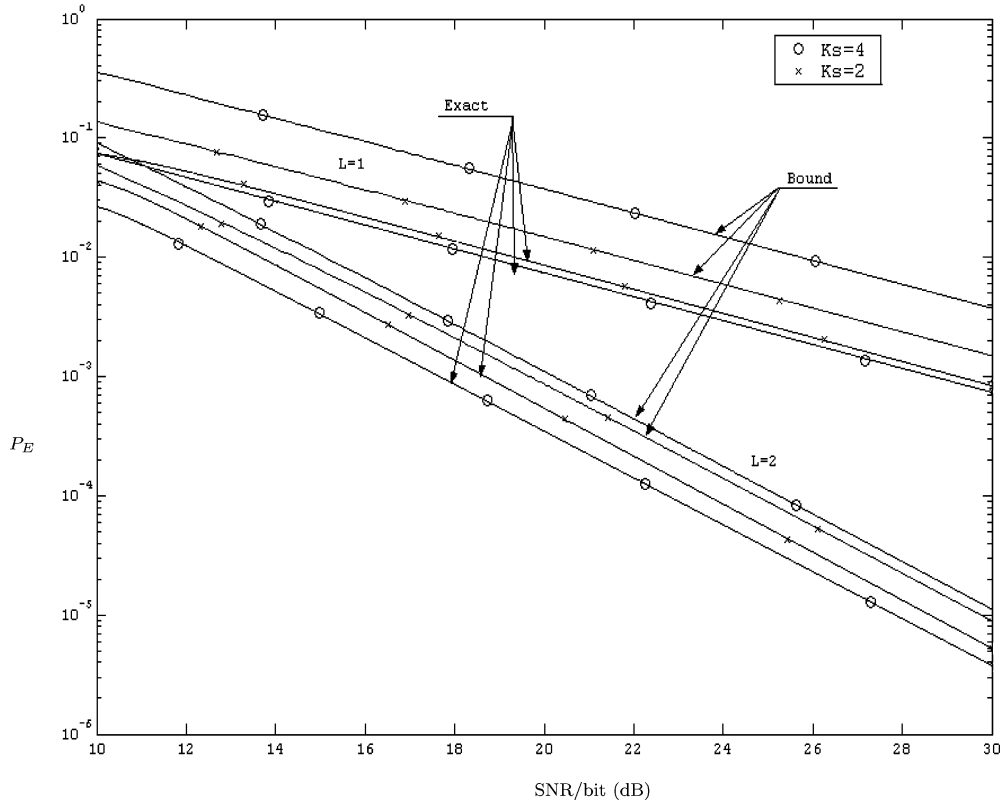

Fig. 7. Comparison of the exact evaluation and upper union bounds on the symbol error probability versus average SNR per bit for the conventional MFSK system with $M = 4, 16$, $L = 1, 2$ and $m = 1$.

required SNR per bit to achieve a given error probability) and bandwidth efficiency (R_b/W which is in bit/s/Hz). The comparison between MT-MFSK and MFSK, based on the bandwidth efficiency R_b/W versus $\bar{\rho}_b$ required to achieve a symbol error probability of 10^{-6} in Nakagami channel with $m = 1$ and $L = 2$, are tabulated in Table III. The average SNR per bit of MFSK required to achieve a symbol error probability of 10^{-6} are calculated by using [5, eq. (18)], which are exact values. From the data in Table III, we observe that MT-MFSK signals can perform better than the conventional MFSK system in terms of power efficiency and bandwidth efficiency.

Since conventional MFSK is a special case of MT-MFSK signals (for $w = 1$, $l_N = M - 1$, and $l_I = 0$), a comparison of the union bound in (61) with the exact error probability for the conventional MFSK signaling and SLC of the L diversity signals, which was given by [5, eq. (18)] reveals the tightness of the bound. Fig. 7 illustrates this comparison when the diversity channels are mutually statistically independent. We observe that the union bound is quite weak in the fading channels. The bound increases as $k_s = \log_2 M$ increases, whereas the exact symbol error probability decreases with increasing k_s. Furthermore, for a given k_s, the bound decreases and become more tight as the diversity branches L increases. Also, for a given k_s and L, the bound decreases with increasing fading parameter m.

A careful observation of the MT-MFSK system reveals that, to represent k_s-bits per symbol, while MT-MFSK system uses only v possible modulated frequencies. This number of frequencies is less than that used by the conventional MFSK system (see Table I). Therefore, for transmitting the same number of bits per symbol, an MT-MFSK system which provides power gain over a conventional MFSK system is not necessarily more complex than MFSK.

VI. Conclusion

In this paper, a mathematical model of MT-MFSK signals based on BIB-design was presented. Such signals are characterized by their ability to increase the signal volume without increasing the number of tones required to represent $M = 2^{k_s}$ waveform, as in the case of the conventional MFSK systems. This means less complexity and less bandwidth for the same bit rate, and thereby allowing higher bandwidth efficiency. The performance of MT-MFSK signals with postdetection noncoherent diversity reception over slow nonselective arbitrarily correlated and unbalanced Nakagami-m fading channels has been considered, in which the diversity branches can have different SNRs, as well as different severity parameter m. A noncoherent SLC soft-decision receiver for MT-MFSK signals has been introduced. The probability of error was analyzed, and a union-bound on the symbol error rate has been obtained. The results show that noncoherent MT-MFSK with diversity creates a multiplicative diversity of order $L(w-1)$ and, therefore, performs better than the conventional MFSK system with relatively less complexity and higher bandwidth efficiency. It was shown that for a given error rate and as the number of diversity levels increased, significant performance gain could be achieved compared with an equivalent nondiversity system. Significant performance gain is also achieved compared with the conventional MFSK system for a given bit-error rate and using the same number of diversity levels.

REFERENCES

[1] S. Stein, "Fading channel issues in system engineering," *IEEE J. Select. Areas Commun.*, vol. SAC-5, no. 2, pp. 68–88, Feb. 1987.

[2] M. K. Simon and M. S. Alouini, "Bit error probability of noncoherent M-ary orthogonal modulation over generalized fading channels," *J. Commun. Netw.*, vol. 1, pp. 111–117, Jun. 1999.

[3] M. Z. Win and R. K. Mallik, "Error analysis of noncoherent M-ary FSK with postdetection EGC over correlated Nakagami and Rician channels," *IEEE Trans. Commun.*, vol. COM-50, pp. 378–383, Mar. 2002.

[4] Q. T. Zhang, "Error performance of noncoherent MFSK with L-diversity on correlated fading channels," *IEEE Trans. Wireless Commun.*, vol. 1, pp. 531–539, Jul. 2002.

[5] I. Ghareeb and M. Abu-Sbeih, "Performance of MFSK signals with postdetection square-law diversity combining in arbitrarily correlated Nakagami-m fading channels," *IEEE Commun. Lett.*, vol. 8, no. 2, pp. 108–110, Feb. 2004.

[6] J. K. Karlof and Y. O. Chang, "Optimal permutation codes for the Gaussian channel," *IEEE Trans. Inf. Theory.*, vol. IT-43, pp. 356–358, Jan. 1997.

[7] W. W. Peterson, "A note on permutation modulation," *IEEE Trans. Inf. Theory*, vol. IT-43, no. 1, pp. 359–360, Jan. 1997.

[8] J. F. Pieper, J. G. Proakis, R. R. Reed, and J. K. Wolf, "Design of efficient coding and modulation for Rayleigh-fading channels," *IEEE Trans. Inf. Theory*, vol. IT-24, pp. 457–468, Jul. 1978.

[9] G. E. Atkin and H. P. Corrales, "An efficient modulation/coding scheme for MFSK systems on bandwidth constrained channels," *IEEE J. Sel. Areas Commun.*, vol. SAC-7, no. 9, pp. 1396–1401, Dec. 1989.

[10] M. J. Evans and K. W. Yates, "Symbol and carrier phase synchronization of MT-MFSK symbols," *Electron. Lett.*, vol. 29, pp. 1304–1305, 1993.

[11] ——, "Optimum harmonic spacing for MT-MFSK synchronization symbols," *Electron. Lett.*, vol. 30, pp. 543–544, Mar. 1994.

[12] X. Giraud, E. Boutillon, and J. C. Belfiore, "Algebraic tools to build modulation schemes for fading channels," *IEEE Trans. Inf. Theory*, vol. 43, no. 3, pp. 938–952, May 1997.

[13] M. Hall, Jr., *Combinatorial Theory*. New York: Wiley, 1986.

[14] F. G. McWilliams and N. J. Sloane, *The Theory of Error Correcting Codes*, 6th ed. Amsterdam, The Netherlands: North-Holland, 1988.

[15] E. S. Kramer and M. D. Mesner, "Admissible parameters for Steiner systems $S(t, k, v)$, with a table for all $(t' - t) \leq 498$," *Utilitas Mathematica*, vol. 7, pp. 221–222, 1975.

[16] M. Nakagami, "The m distribution—A general formulas for intensity distribution of rapid fading," in *Statistical Methods in Radio Wave Propagation*, W. G. Hoffman, Ed. Oxford, U.K: Pergamon, 1960, pp. 3–36.

[17] J. G. Proakis, *Digital Communications*, 3rd ed. New York: McGraw-Hill, 1995.

[18] P. M. Hahn, "Theoretical diversity improvement in multiple frequency-shift keying," *IRE Trans. Commun. Syst.*, vol. 50, pp. 177–184, Jun. 1962.

[19] I. S. Gradshteyn and I. M. Ryzhik, *Table of Integrals, Series, and Products*. New York: Academic, 1980.

[20] A. Papoulis and S. U. Pillai, *Probability, Random Variables and Stochastic Processes*, 4th ed. New York: McGraw-Hill, 2002.

[21] P. Lombardo, G. Fedele, and M. M. Rao, "MRC performance for binary signals in Nakagami fading with general branch correlation," *IEEE Trans. Commun.*, vol. 47, no. 1, pp. 44–52, Jan. 1999.

Ibrahim Ghareeb (M'98) received the B.Sc. degree from Yarmouk University, Irbid, Jordan, in 1985, the M.Sc. degree from Jordan University of Science and Technology, Irbid, in 1988, and the Ph.D. degree from the University of Ottawa, Ottawa, ON, Canada, in 1995, all in electrical engineering.

From 1988 to 1991, he worked as an Instructor and a System Engineer at the Ministry of Higher Education, Jordan. In 1995, he joined the Electrical Engineering Department, Jordan University of Science and Technology, where he is currently a member of the Center for Wireless Communications and Internet Technology, Jordan University of Science and Technology. In 1997, he spent the summer term as a Research Associated at the University of Ottawa. His area of research include digital communications with emphasis on digital modulation techniques, error control coding, wideband mobile and indoor wireless communications, multiple access for wireless high-speed communications, spread spectrum, and MIMO communication systems. He collaborates closely with the local industry and research institutions. He has been active in organizing several international conferences on communications.

Dr. Ghareeb is a Professional Engineer in Jordan.